



Heart Muscle Microphysiological System for Cardiac Liability Prediction of Repurposed COVID-19 Therapeutics

B er n ce Charrez^{1†}, Verena Charwat^{1†}, Brian A. Siemons¹, Ishan Goswami¹, Courtney Sakolish², Yu-Syuan Luo², Henrik Finsberg³, Andrew G. Edwards⁴, Evan W. Miller^{5,6,7}, Ivan Rusyn² and Kevin E. Healy^{1,8*}

¹Department of Bioengineering and California Institute for Quantitative Biosciences (QB3), University of California at Berkeley, Berkeley, CA, United States, ²Department of Veterinary Integrative Biosciences, College of Veterinary Medicine and Biomedical Sciences, Texas A&M University, College Station, TX, United States, ³Simula Research Laboratory, Oslo, Norway, ⁴Department of Pharmacology, School of Medicine, University of California at Davis, Davis, CA, United States, ⁵Department of Chemistry, University of California at Berkeley, Berkeley, CA, United States, ⁶Department of Molecular and Cell Biology, University of California at Berkeley, Berkeley, CA, United States, ⁷Helen Wills Neuroscience Institute, University of California at Berkeley, Berkeley, CA, United States, ⁸Department of Materials Science and Engineering, University of California at Berkeley, Berkeley, CA, United States

OPEN ACCESS

Edited by:

Deok-Ho Kim,
Johns Hopkins University,
United States

Reviewed by:

Michele Samaja,
University of Milan, Italy
Tim Kacprowski,
Technische Universit t Braunschweig,
Germany

*Correspondence:

Kevin E. Healy
kehealy@berkeley.edu

[†]These authors have contributed
equally to this work and share first
authorship

Specialty section:

This article was submitted to
Translational Pharmacology,
a section of the journal
Frontiers in Pharmacology

Received: 23 March 2021

Accepted: 05 July 2021

Published: 04 August 2021

Citation:

Charrez B, Charwat V, Siemons BA,
Goswami I, Sakolish C, Luo Y-S,
Finsberg H, Edwards AG, Miller EW,
Rusyn I and Healy KE (2021) Heart
Muscle Microphysiological System for
Cardiac Liability Prediction of
Repurposed COVID-19 Therapeutics.
Front. Pharmacol. 12:684252.
doi: 10.3389/fphar.2021.684252

Despite global efforts, it took 7 months between the proclamation of global SARS-CoV-2 pandemic and the first FDA-approved treatment for COVID-19. During this timeframe, clinicians focused their efforts on repurposing drugs, such as hydroxychloroquine (HCQ) or azithromycin (AZM) to treat hospitalized COVID-19 patients. While clinical trials are time-consuming, the exponential increase in hospitalizations compelled the FDA to grant an emergency use authorization for HCQ and AZM as treatment for COVID-19, although there was limited evidence of their combined efficacy and safety. The authorization was revoked 4 months later, giving rise to controversial political and scientific debates illustrating important challenges such as premature authorization of potentially ineffective or unsafe therapeutics, while diverting resources from screening of effective drugs. Here we report on a preclinical drug screening platform, a cardiac microphysiological system (MPS), to rapidly identify clinically relevant cardiac liabilities associated with HCQ and AZM. The cardiac MPS is a microfabricated fluidic system in which cardiomyocytes derived from human induced pluripotent stem cells self-arrange into a uniaxially beating tissue. The drug response was measured using outputs that correlate with clinical measurements such as action potential duration (proxy for clinical QT interval) and drug-biomarker pairing. The cardiac MPS predicted clinical arrhythmias associated with QT prolongation and rhythm instabilities in tissues treated with HCQ. We found no change in QT interval upon acute exposure to AZM, while still observing a significant increase in arrhythmic events. These results suggest that this MPS can not only predict arrhythmias, but it can also identify arrhythmias even when QT prolongation is absent. When exposed to HCQ and AZM polytherapy, this MPS faithfully reflected clinical findings, in that the combination of drugs synergistically increased QT interval when compared to single drug exposure, while not worsening the overall frequency of arrhythmic events. The high content cardiac MPS can

rapidly evaluate the cardiac safety of potential therapeutics, ultimately accelerating patients' access to safe and effective treatments.

Keywords: microphysiological systems, induced pluripotent stem cells, heart muscle, cardiomyocytes, SARS-CoV-2, hydroxychloroquine, azithromycin, polytherapy

INTRODUCTION

With the high incidence of COVID-19 cases worldwide, almost 120 million people have tested positive, leading to more than 3.7 million deaths by June 2021 (JHU, 2020). Global deployment of vaccines remains a challenge that may take as long as 12 months to address (Burgos et al., 2021; Randall, 2021). It is therefore critical to continue to treat COVID-19 patients with appropriate therapeutics, some of them repurposed from other clinical indications. Early clinical trials identified hydroxychloroquine (HCQ) and azithromycin (AZM) as promising therapeutics to help treat or reduce the effects of SARS-CoV-2 (Gautret et al., 2020; Huang et al., 2020; Wang et al., 2020; Yao et al., 2020). On March 28th, 2020 the FDA granted an emergency use authorization for oral administration of HCQ as treatment against COVID-19 (FDA, 2020a). In early June 2020 the FDA cautioned the use of HCQ for COVID-19 treatment outside of hospital settings due to the reported risk of heart complications (FDA, 2020b). The authorization for HCQ and AZM was revoked on June 22, 2020, largely due to the lack of evidence for their effectiveness in COVID-19 patients and the risk of side effects (Furtado et al., 2020; Gérard et al., 2020; Molina et al., 2020; Rosenber et al., 2020; Self et al., 2020). This sequence of events was politically and scientifically controversial and illustrated important challenges that can arise with emergency drug authorizations during crises, notably the authorization of potentially ineffective or unsafe therapeutics, while diverting resources from screening of effective drugs (Thomson and Nachlis, 2020). Close to 250 clinical trials were started to study the efficacy of HCQ treatment for COVID-19, 80 of them a polytherapy by combining HCQ with the antibiotic AZM. Only 11 polytherapy trials were completed, while several trials were terminated due to adverse cardiac side effects associated with the treatments (Andrea Natale, 2020; Rupesh Agrawal, 2020). Although the FDA has recently approved other therapeutics for the treatment of COVID-19, such as the anti-viral remdesivir (FDA, 2020c), the World Health Organization (WHO) withdrew its approval a month later (World Health Organization, 2020). Clearly, there is an urgent need for *in vitro* screening tools to increase the speed and precision of pre-clinical evaluation of potential COVID-19 therapeutics so that clinical resources can be focused on the most promising candidates.

To address this need, in this study, we show the clinically predictive potential of a microphysiological system (MPS; also called organ-on-a-chip) for rapid screening of cardiac liabilities associated with repurposed drug polytherapy. We chose the heart as a tissue of interest because all drugs need to be screened for cardiac liabilities such as arrhythmias, tachycardia, QT prolongation, and Torsade's de pointes (TdP), all of which can

lead to sudden cardiac arrest. Furthermore, as recent studies have shown that SARS-CoV-2 infections can damage the heart's contractile proteins (Perez-Bermejo et al., 2020), and cardiac comorbidities increase the likelihood of hospitalization and death (Nishiga et al., 2020; Sanyaolu et al., 2020; Ssentongo et al., 2020), there is an urgency for rapid drug screening tools predictive of clinical cardiology. Our cardiac MPS is a microfabricated fluidic system, that promotes human induced pluripotent stem cell-derived cardiomyocytes (hiPSC-CMs) to self-arrange into an organized, three-dimensional beating cardiac muscle fiber (Mathur et al., 2015). We further enhance the prognostic capability of our system by exposing the tissues to an in-house developed maturation media, leading to pharmacology outcomes more reminiscent of adult drug response (Huebsch et al., 2020). The drug response from the cardiac MPS can be further matured and analyzed *via* computational approaches (Tveito et al., 2018; Jæger et al., 2020a; Jæger et al., 2020b).

We chose HCQ and AZM as an example of polytherapy approved by the FDA for emergency use as treatment of COVID-19. We have previously used the heart muscle MPS platform in a mock *in vitro* clinical trial, successfully predicting clinical trial outcomes for HCQ and AZM polytherapy (Charrez et al., 2021). This chronic experiment was performed over 10 days to replicate clinical trial protocols. Our focus in this work was to conduct acute dose escalation studies of HCQ and AZM, and their polytherapy to demonstrate the platform's ability to identify dosing regimens that alleviate cardiac liabilities. To address rapid cardiotoxic screening, a novel 4-plex version of our cardiac MPS was employed for drug dose escalation studies. We used multiple metrics to assess the pro-arrhythmic risks of HCQ and AZM polytherapy. We measured beat rate corrected action potential duration prolongation (cAPD) as a proxy for clinical QT prolongation, changes in the beat waveform (triangulation), action potential and calcium transient maximum upstroke velocity, and the occurrence of early after depolarizations (EADs) and delayed after depolarizations (DADs) as a function of dose, to identify the cardiac risk for each drug tested. Employing a voltage sensitive dye and hiPSC-CMs with a genetically encoded calcium reporter, we obtained precise APD and calcium transient outcomes of the cardiac muscle tissues as they were treated with HCQ and AZM.

We identified a QT increase in HCQ treated tissue, and its correlation to arrhythmic events, consistent with retrospective studies (Sharma et al., 2016; Blinova et al., 2017; Jankelson et al., 2020) and clinical literature (Asensio et al., 2020; Bessière et al., 2020). Our cardiac MPS showed no change in QT interval upon acute exposure to AZM, while observing a significant increase in arrhythmic events, indicating that the cardiac MPS predicted arrhythmias even in the absence of QT prolongation

(Yang et al., 2017). Polytherapy showed a synergetic increase of QT interval when compared to monotherapy treatments. This observation was in line with literature data that reported a worsening of QT interval increase with the combination therapy (Chorin et al., 2020a; Chorin et al., 2020b; Bessière et al., 2020; Mercurio et al., 2020). Finally, proteomics analysis of effluent enabled the discovery of biomarkers that were directly correlated with cardiotoxicity and cellular damage. The outcomes of this paper correlate with published clinical results, validating our cardiac MPS as a good and rapid predictor of drug-induced arrhythmias.

MATERIALS AND METHODS

Fabrication of Cardiac Microphysiological System

Microfluidic cardiac MPS were formed using an optimized version of the protocol described in our previous work (Mathur et al., 2015; Huebsch et al., 2020). Each MPS consisted of four multiplexed cell-loading port leading to their respective cell culture chambers (1300 $\mu\text{m} \times 130 \mu\text{m}$) and two media ports, one media inlet and outlet per MPS. The media channels run adjacent to each side of the four cell chambers, separated by an array of fenestrations (2 $\mu\text{m} \times 2 \mu\text{m}$ high/width) to deliver nutrients while protecting the tissue from media flow shear stress. Two step photolithography was used to fabricate the microdevice silicon wafer mold, containing the features of multiple MPS. The first photolithography step was 2 μm high for the fenestration pattern: The piranha cleaned wafer was put onto a headway spinner where SU8 2002 (Kayaku Advanced Materials, Westborough, MA) was poured and spun (first 500 rpm for 10 s with 100 rpm/s acceleration; then 2000 rpm for 30 s with 300 rpm/s acceleration). The wafer was baked for 1 min at 95°C, exposed at 80 mJ/cm² UV exposure (Karl Suss MA6 mask aligner with i-line) and baked again for 2 min at 95°C. Non-crosslinked photoresist was developed in SU8 developer for 1 min 15 s, and the wafer was hard baked at 180°C for 30–45 min. The second layer for cell chamber and media channel (55 μm high) could then be fabricated onto of the fenestration with a similar protocol. SU8 3050 (Kayaku Advanced Materials) was used and spun (first 500 rpm for 10 s with 100 rpm/s acceleration; then 3000 rpm for 30 s with 300 rpm/s acceleration). The wafer was baked slowly to allow for improved resolution: starting at 30°C, the temperature was increased to 65°C at a rate of 10°C/min. Once at 65°C, the temperature was kept for 10 min before ramping up to 95°C at a rate of 5°C/3 min. Wafers were kept at 95°C for 45 min. The wafer was then allowed to cool down slowly to room temperature before being exposed to UV at 160 mJ/cm². Alignment marks allowed for perfect overlay of both layers. Post exposure bake was the same as previously described, with only 2 min at 65°C and 10 min at 95°C. Finally, wafers were developed for 35 min in shaker and sonicator before being hard baked at 180°C for 30–45 min. The cardiac MPS was formed by replica molding from the silicon wafer with polydimethylsiloxane (PDMS; Sylgard 184 kit, Dow Chemicals, Midland, MI) at a 10:1 ratio of Sylgard base to crosslinker. PDMS chips were then

bonded to glass slides using oxygen plasma for 24 s, RF power 21W, and 100% oxygen flow.

Fluid Dynamic Modeling

Microfluidic cardiac Characterization of fluid flow and wall shear stresses in the cardiac MPS was done *via* solving the Navier-Stokes equation using the finite element solver, COMSOL Multiphysics® (v 5.4, COMSOL, Inc. Burlington, MA). The computational domain was constructed by importing the geometry of the fluidic channels of the MPS. Fluid was modeled to be Newtonian and incompressible with a density of 1 g/mL and a dynamic viscosity of 1 mPa-s, and the flow within the fluidic channels were assumed to be laminar. Inlet boundary condition was set to mass-influx (based on the design flowrate of 30 $\mu\text{L}/\text{min}$) and outlet boundary condition was set to a gauge pressure of 0 Pa. For all other boundaries (i.e. walls), no-slip conditions were applied. Discretization of the computational domain was performed using the physics driven extra fine mesh. Steady state solver was used to obtain the velocity as well as the wall shear stress profiles within the MPS.

Cell Source

Wild type C (WTC) hiPSC was used for this study. The cell line has a single-copy of CAG-driven GCaMP6f knocked into the first Exon of the AAVS1 “safe harbor” locus (Huebsch et al., 2015). It can be purchased from the Coriell Repository (# GM25256 hiPSC from fibroblast).

Cardiomyocyte Differentiation

WTC hiPSC were differentiated to cardiomyocytes (CM) through small molecular manipulation of Wnt signaling pathway (Lian et al., 2013; Lian et al., 2014; Dunn and Palecek, 2018). Canonical Wnt ligands promote cell fate determination during embryonic development *via* inhibition of glycogen synthase kinase 3 (Gsk3) with CHIR99021. A decrease in Gsk3 expression leads to the nuclear accumulation of β -catenin and the subsequent activation of cardiac differentiation genes transcription machinery. To obtain fully differentiated CM, an inhibitor of Wnt (IWP4) is used to stop Wnt protein secretion and activity by preventing the palmitoylation of Wnt proteins by Porcupine. Thawed hiPSCs were passaged three times at a density of 20,000 cells/cm² in mTeSR-1 media (StemCell Technologies, Vancouver, Canada) with 10 μM Y27632 (Peprtech; Rocky Hill, NJ). After 3 days of expansion the differentiation was initiated. At day 0, the >90% confluent hiPSC wells were exposed to 8 μM CHIR99021 (Peprtech) in Roswell Park Memorial Institute (RPMI) 1640 medium containing B-27 supplement without insulin (RPMI-I). The next day, cells were fed with RPMI-I only. On day two, cells were exposed to 5 μM IWP-4 (Peprtech) and 150 $\mu\text{g}/\text{mL}$ L-ascorbic acid (LAA) in RPMI-I for 2 days. On day four, cells were fed with RPMI-I only for two more days. From then onwards, RPMI containing standard B-27 supplement with insulin (RPMI + C) was added every second day. Typically, CM start beating on day eight of differentiation. After 15 days, hiPSC-CM were singularized with collagenase type II (Worthington Biochemical Corporation, Lakewood, NJ) for 45–60 min at 37°C and subsequently plated at a density of

TABLE 1 | Drug and doses used for both acute and chronic exposure.

Drug	Primary purpose	Clinical C _{max}	Acute drug dose (*C _{max})
Hydroxychloroquine—HCQ (<i>PHR1782-1G, Sigma</i>)	Anti-malarial	1 μM Yao et al. (2020)	0, 0.1, 1, 10, 100, 1000
Azithromycin—AZM (<i>75,199-25 MG-F, Sigma</i>)	Macrolide antibiotic	0.67 μM Gautret et al. (2020)	0, 0.1, 1, 10, 100
HCQ + AZM combination	SARS-CoV2	—	HCQ: 0, 1, 1, 1, 1, 1, 1 AZM: 0, 0, 0.1, 0.3, 1, 3, 10

100,000 cells/cm² onto Matrigel, in EB20 with 10 μM Y27632 (new “day 0” after replating) (Huebsch et al., 2020). The next day, medium was exchanged for RPMI + C. At day three, cells were fed with RPMI 1640 [no glucose, with pyruvate supplemented with 23 mM sodium bicarbonate and 4 mM Sodium L-lactate (Tohyama et al., 2013)] for a total of 4 days (exchanged every other day) to allow for cardiomyocytes only to survive. At day seven, cells were washed with dPBS and fed with RPMI + C to recover. Two days after that, cardiomyocytes were singularized, and a fraction of them was characterized by flow cytometry for Cardiac Troponin T, and the remaining cells were loaded into cardiac MPS. Only differentiations with >95% cells positive for Cardiac Troponin T were subsequently loaded in the MPS.

Loading of Cardiomyocytes and Microtissues Assembly Within Microphysiological System

Singularized- lactate-purified WTC hiPSC-derived cardiomyocytes were suspended in EB20 media supplemented with 10 μM Y27632. Density was calculated so that 3 μL of the cell suspension corresponded to 4,000 cells, that were injected into the loading port of each MPS. After 3 min centrifugation at 300 g, MPS were inspected under the microscope. Chambers that were not filled at this point were discarded. MPS were fed with 200 μL EB20 media supplemented with 10 μM Y27632 into the inlet tip and gravity would allow for a constant flow to the outlet until equilibrium was reached. The following day and every other day from then on, media was changed to our in-house “Maturation Media” (MM) as described in (Huebsch et al., 2020). MPS tissues were allowed to mature for 10 days before any subsequent experiments were performed.

Pharmacology Studies

Twenty-four hours prior to any experiment, MPS tissues were stained with 500 nM of the action potential dye, BeRST-1, synthesized and quality controlled as described by Miller et al. (Huang et al., 2015). On the day of pharmacology study, drugs were weighed and dissolved in maturation media (MM) with 50 nM BeRST-1 voltage dye and adjusted vehicle concentration: all AZM doses had the same solvent conc. 0.5% EtOH. Hydroxychloroquine Sulfate (PHR1782-1G, Sigma, St. Louis, MO) was dissolved in PBS at 4.34 mg/mL and sterile filtered to create a 10 mM stock solution. The stock was always prepared fresh at the day of the experiment. Azithromycin (75199-25 MG-F, Sigma) was dissolved in 100% ethanol to create a 10 mg/mL (=13.35 mM) stock. The stock was stored at -20°C for up to 3 days. From the stock concentration, drugs were diluted to the highest dose tested and serial dilutions were made up to the

lowest concentration range. Doses were chosen to vary around clinical C_{max} of HCQ at 1 μM (Yao et al., 2020) and AZM at 0.67 μM (Gautret et al., 2020) (Table 1). Once the drug solutions were freshly prepared, MPS were placed onto a heated plate (Tokai Hit, Gendoji-cho, Japan) at 37°C for 20 min to let them stabilize. Their action potential was recorded and only tissues with APD<500 ms were selected for study. Seven tissues per drug were used for the studies. A pressure driven pump system (Fluigent, N. Chelmsford, MA) comprising a 10-way selection valve (M-switch) and flow sensor (size M) was used for controlled and automated perfusion of increasing drug doses through the cardiac MPS. The flow sensor enabled a regular flow of 30 μL/min throughout the experiment. **Supplementary Figure 1** for a schematic of the setup. When two microfluidic chips were hooked up in parallel, micrometering needle valves were included downstream of the MPS to adjust for equal flow into both sides. Each chip housed four tissue chambers (Figure 1). Once the tissues were selected based on their inclusion criteria (APD<500 ms and good visual quality), the fresh drug solutions were added to the Fluigent system. The tubing was primed with the different drug doses and the MPS inlet was connected to the Fluigent system outlet. The MPS outlet tubing was connected to an eppendorf for effluent collection. Alligator clips, connected to a Myopacer Field Simulator (IONOPTIX, Westwood, MA), were attached to the stainless-steel elbows (SC20/15 bent to 90°, Instech Laboratories, Plymouth Meeting, PA) of the MPS inlet and outlet to pace the tissues. Once the whole system was setup, with constant 30 μL/min flowrate through the MPS, the tissues were left for 30 min to stabilize. At this point, initial dose 0 recordings of spontaneous and paced activity were performed. The pump M-switch was then changing its output to the lowest drug dose, dose 0 effluent tube was replaced by an empty tube. MPS were incubated for 30 min. Spontaneous and paced activity was then recorded for the first dose and the process was iterated for increasing doses until all spontaneous and paced activity ceased or the highest dose was reached.

Image Acquisition for Pharmacology Studies

Initial spontaneous recordings were the following: 6- and 30-s videos of fluorescent calcium flux as well as 6-s voltage dye videos. After that, the tissues were field paced at 1 or 1.5 Hz. Since the multiplex design has four tissue for one media inlet and outlet, all tissues were paced at the same frequency. Tissues were paced at 1 Hz, and if at least one of the four tissues did not capture the 1 Hz pacing the frequency was increased to 1.5 Hz. The same frequency was kept for the entire drug dose escalation study. For each recording, tissues were paced for 10 s (3 V, 20 msec

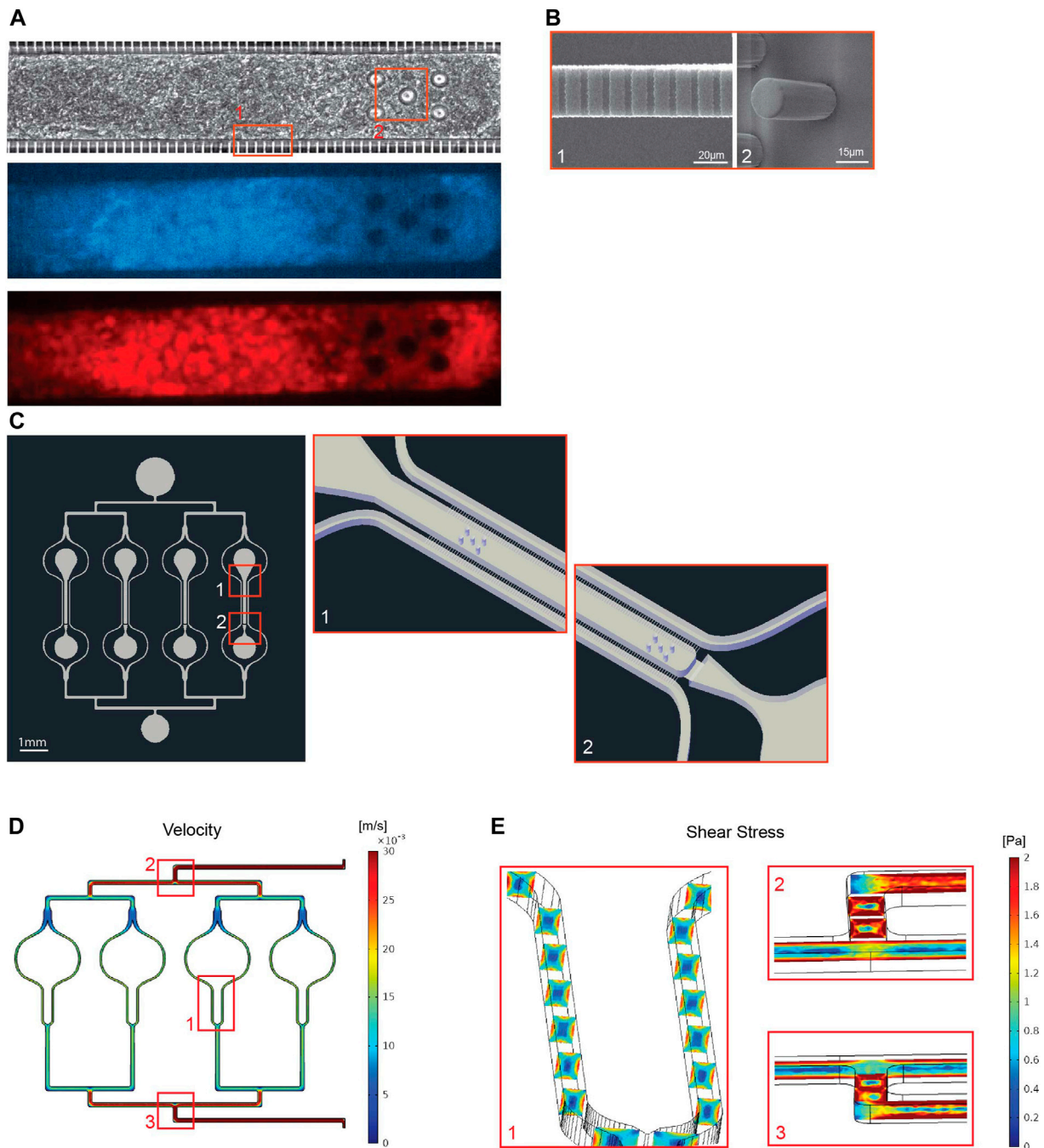
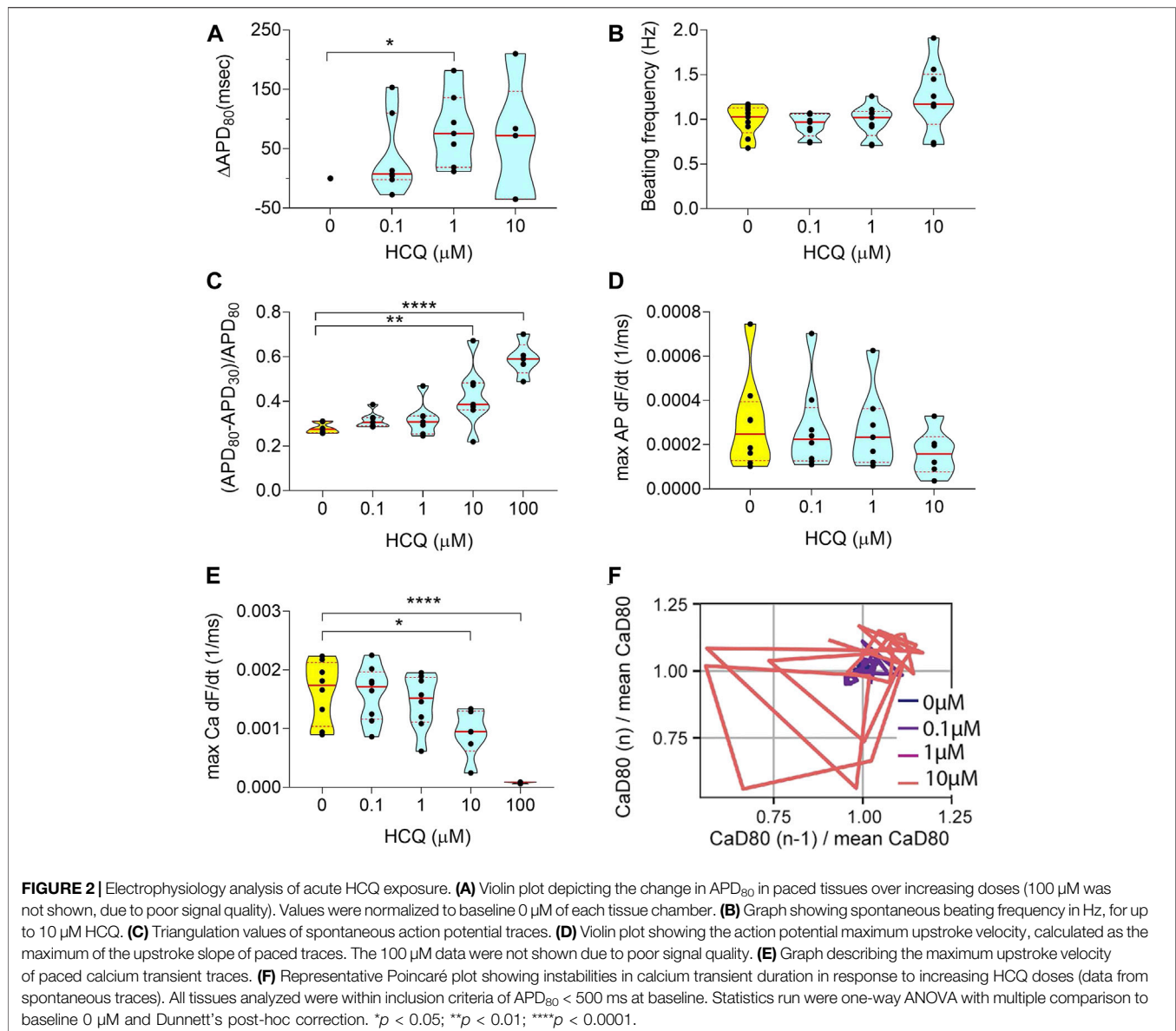


FIGURE 1 | Design of the multiplexed cardiac microphysiological system (MPS). **(A)** 20x images of a cardiac MPS loaded with 4,000 human induced pluripotent stem cell derived cardiomyocytes. Top image shows brightfield capture of the tissue, middle image shows GFP fluorescence for calcium transient recordings, and bottom shows FarRed fluorescence of the voltage dye staining. **(B)** To left SEM image shows the fenestrations ($2\mu\text{m} \times 2\mu\text{m} \times 20\mu\text{m}$: h-w-l) required for protecting tissue in the cell chamber from media flow-induced shear stress (panel **E**) while enabling diffusion of nutrients. The right SEM image is a close up on pillars that keep the tissue fiber spanned along the length of the cell chamber. Both images correspond to area from panel (A) denoted by one and two respectively. **(C)** Illustration of the 4-plex tissue chamber MPS (left) and a three dimensional schematic (right) of top (1) and bottom (2) portions of one tissue chamber, which dimensions were $1300\mu\text{m} \times 130\mu\text{m}$ with five $20\mu\text{m}$ diameter pillars of at the top and the bottom of the chamber. **(D)** Illustration of the fluidics velocity profile obtained with COMSOL Multiphysics for volume flow rate of $30\mu\text{L}/\text{min}$, ranging from $30\text{mm}/\text{s}$ at the inlet and dropping to $16\text{mm}/\text{s}$ equally around each cell chamber. **(E)** Close up showing shear stress profiles in the media channels around the cell chamber (1), at the first (2) and last (3) bifurcation of the multiplex chip.



bipolar pulses) *via* stainless steel elbow fluidic connectors inserted in both the media inlet and outlet. Pacing was maintained while 6 s calcium and voltage videos were acquired. Once spontaneous and paced recordings were performed, MPS were exposed to higher drug concentration, incubated for 30 min before the next recording sequence was started. A NIKON TE300HEM microscope with a HAMAMATSU digital CMOS camera C11440/ORCA-Flash 4.0 was used and enabled 100 frames per second videos. For fluorescence imaging, a Lumencor (Beaverton, OR) SpectraX Light Engine and filtered with a QUAD filter (Semrock (IDEX), Rochester, NY) was used. GCaMP videos used the Cyan LED, 470 nm (4×4 binning, 10 ms), while BeRST-1 videos used the Far-red LED, 640 nm (4×4 binning, 10 ms). Videos were acquired using Nikons NIS-Elements software. Post-experiment processing was performed with an in-house

developed Python library that could analyze the fluorescence intensity over the time of the recording.

Thorough Electrophysiology Analysis as a Proxy for Clinical QT Interval Study and Arrhythmia Prediction

Clinically, QT interval increase is often associated with arrhythmias, such as Torsade de Pointes (TdP) (Hondeghe et al., 2001). TdP is a ventricular tachycardia triggered by Early afterdepolarizations (EADs), where the amplitude and configuration of ECG measurements vary continuously. EADs represent a transition from slowed cellular repolarization to unstable (chaotic) repolarization at the cellular level. (Sato et al., 2009; Qu et al., 2013). Patients with QT interval

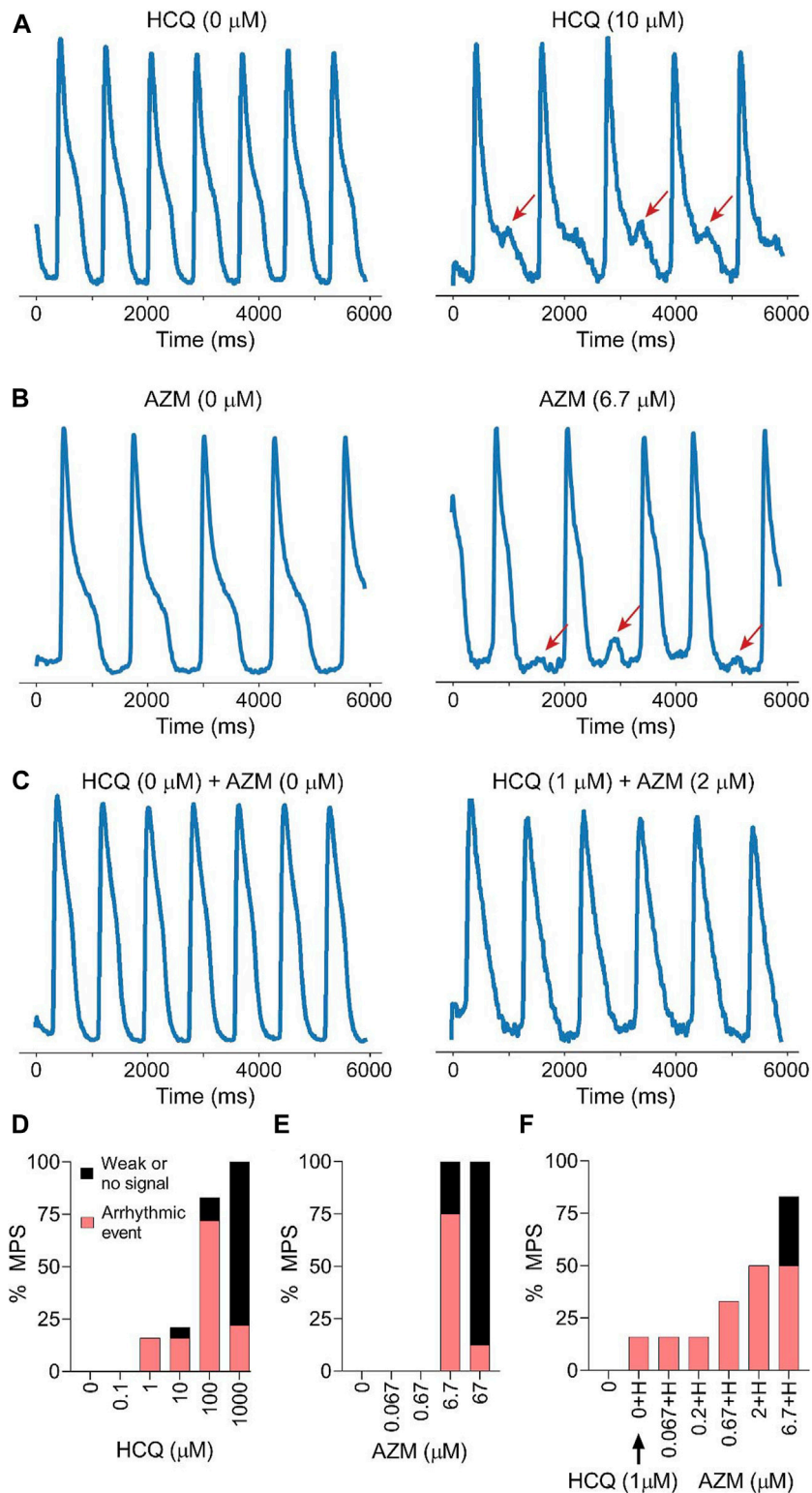


FIGURE 3 | Drug induced arrhythmia for acute HCQ, AZM, and polytherapy. **(A)** Representative calcium transient trace at baseline (**left**) and 10 μM (**right**) HCQ, where early after-depolarization (EAD) can be observed (red arrows). **(B)** Representative calcium transient trace at baseline (**left**) and 6.7 μM (**right**) AZM, where delayed after-depolarization (DAD) can be observed (red arrows). **(C)** Representative calcium transient trace at baseline (**left**) and 1 μM HCQ combined with 2 μM AZM (**right**), where calcium trace amplitude and configuration change. **(D,E,F)** Histogram showing incidence of arrhythmia-like events such as EAD, DAD or irregular beat shape (red) and weak signal or beating cessation (black) as percentage of total MPS for HCQ only **(D)**, AZM only **(E)** and combination therapy **(F)**. Traces used were spontaneous 30 s recording of calcium traces.

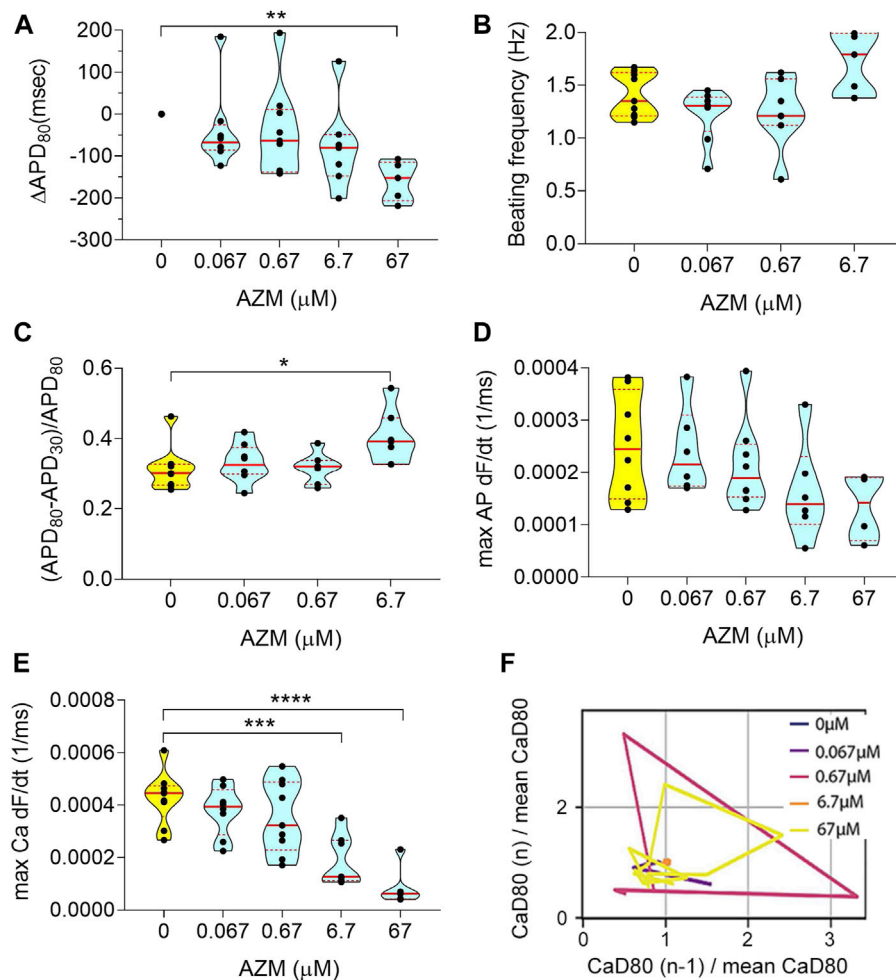


FIGURE 4 | Electrophysiology analysis of acute AZM exposure. **(A)** Violin plot depicting the change in APD_{80} in paced tissues over increasing doses. Values were normalized to baseline $0 \mu\text{M}$ of each tissue chamber. **(B)** Graph showing spontaneous beating frequency in Hz, for up to $6.7 \mu\text{M}$ AZM. At $67 \mu\text{M}$ tissues stopped beating spontaneously and data was therefore excluded from the graph. **(C)** Change in triangulation of spontaneous action potential traces. The $67 \mu\text{M}$ data was not shown, due to cease of spontaneous beating activity. **(D)** Violin plot showing the action potential maximum upstroke velocity, calculated as the maximum of the upstroke slope of paced traces. **(E)** Graph describing the maximum upstroke velocity of paced calcium transient traces. **(F)** Representative Poincaré plot showing instabilities in calcium transient duration in response to increasing AZM doses (data from spontaneous traces). All tissues analyzed were within inclusion criteria of $APD_{80} < 500 \text{ ms}$ at baseline. Statistics run were one-way ANOVA with multiple comparison to baseline $0 \mu\text{M}$ and Dunnett's post-hoc correction. * $p < 0.05$; ** $p < 0.01$; *** $p < 0.001$, **** $p < 0.0001$.

$>500 \text{ ms}$ are considered at risk for TdP (Asensio et al., 2020), therefore all tissues with baseline $APD > 500 \text{ ms}$ were excluded from the study. In this study, we used rate corrected action potential duration at 80% of its repolarization (APD_{80}) as a proxy for QT interval measurements (Blinova et al., 2017). Rate correction was performed with the Fridericia correction (Vandenberk et al., 2016), or by using data from paced tissues. Hondeghem et al. (2001) showed that if APD prolongation was accompanied by instability or triangulation then, EADs and proarrhythmia were more certain to follow. In this study, we defined triangulation as $(APD_{80} - APD_{30})$ normalized to APD_{80} . We also used Poincaré plots to study the instances of instabilities, where the n^{th} APD_{80} is plotted against the $(n-1)^{\text{th}}$ APD_{80} , each normalized to the mean APD_{80} . In the case of stable APD_{80} in successive beats, overlaying traces

at the origin of the graph will be visible (Hondeghem et al., 2001), appearing as a asymmetric circle. However, if there are large deviations between successive APD , large disorganized polygons will be observed that correlate with cardiac arrhythmias. We also characterized arrhythmic instances qualitatively by studying 30 s long calcium traces. EAD, DAD or change in amplitude and shape (loss of plateau phase—typical TdP trait) were considered abnormal ECG and arrhythmic events. If the maximal amplitude of a trace was less than 60% the one of control data, or if no beating was observed, the datapoint was qualified as weak or no beating signal.

Both the action potential and calcium transient maximum upstroke velocity, corresponding to the maximum of the upstroke's slope (max derivative—max dF/dt), is calculated with our in-house Python software.

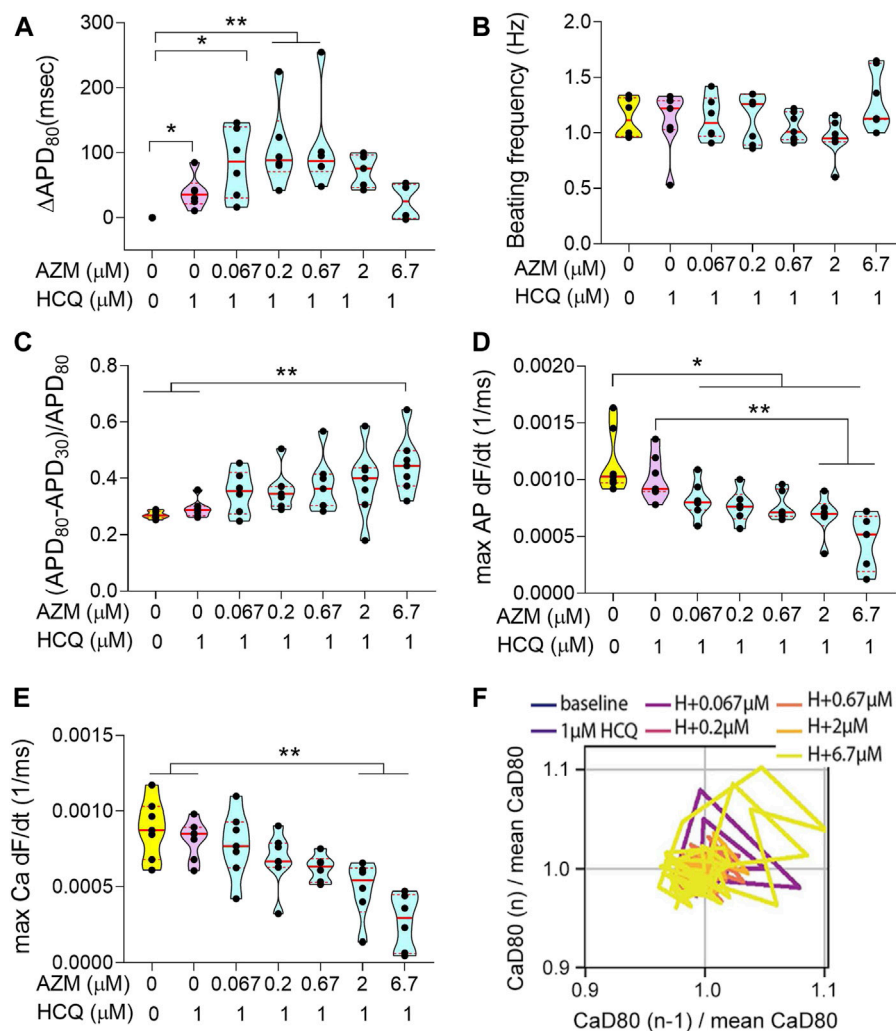


FIGURE 5 | Electrophysiology analysis of acute combination of HCQ and AZM exposure. **(A)** Violin plot depicting the change in APD_{80} in paced tissues over increasing doses. Values were normalized to baseline 0 μM of each respective tissue. **(B)** Graph showing spontaneous beating frequency in Hz. **(C)** Triangulation values of spontaneous action potential traces. **(D)** Violin plot showing the action potential maximum upstroke velocity, calculated as the maximum of the upstroke slope of paced traces. **(E)** Graph describing the maximum upstroke velocity of paced calcium transient traces. **(F)** Representative Poincaré plot showing instabilities in calcium transient duration in response to HCQ + AZM polytherapy (data from spontaneous traces). All tissues analyzed were within inclusion criteria of $APD_{80} < 500$ ms at baseline. Statistics run were one-way ANOVA with multiple comparison to baseline 0 and 1 μM HCQ and Dunnett's post-hoc analysis. Unpaired *t*-test comparison with Welch's correction between 0 and 1 μM HCQ were performed to confirm observations seen in **Figure 2**, *t*-test only showed significance for A. **p* < 0.05; ***p* < 0.01; ****p* < 0.001, *****p* < 0.0001.

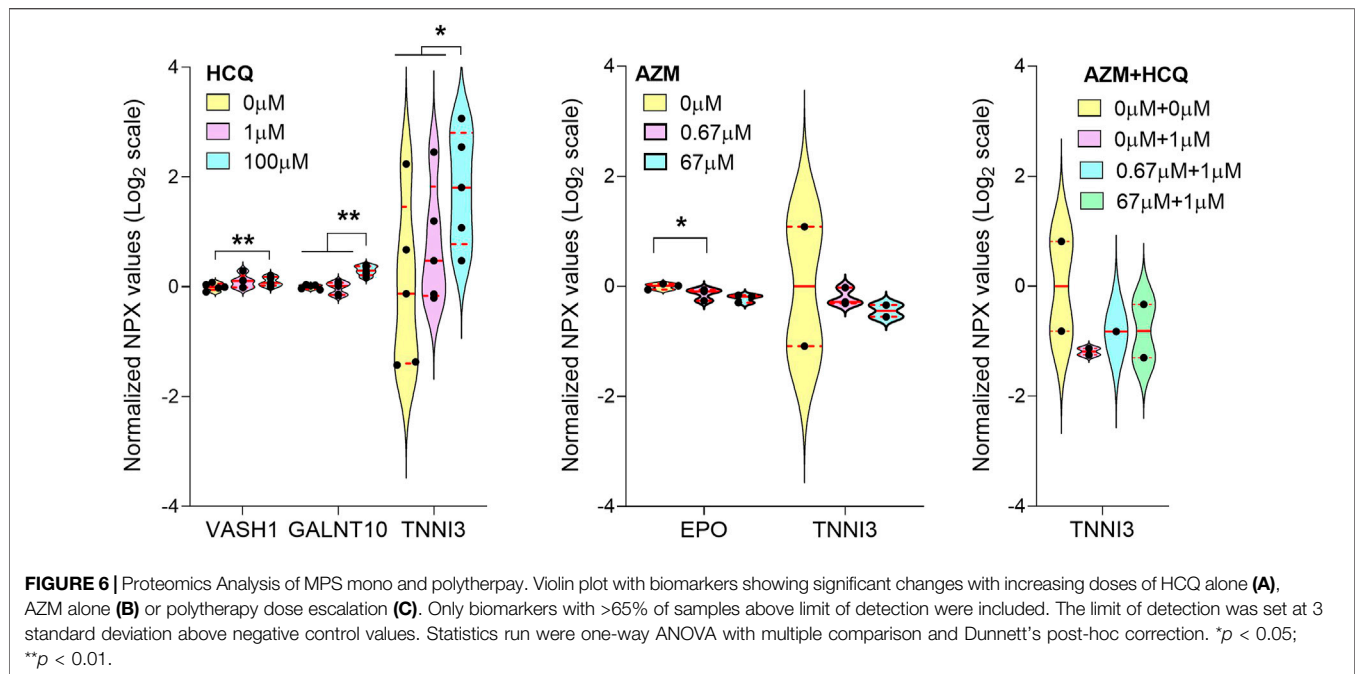
Plasma Protein Profiling Using Olink Multiplex Panel

All effluent samples were kept at -80°C until sent on dry ice and shipped to Olink Proteomics (Watertown, MA) for protein quantification. Olink Proteomics uses multiplex proximity extension assay (PEA) panels (Assarsson et al., 2014), where two matched antibodies labeled with unique DNA oligonucleotides simultaneously bind to a target protein in solution. Their DNA oligonucleotides will hybridize into a double-stranded DNA "barcode" which is unique for the specific antigen and quantitatively proportional to the initial concentration of target protein. The hybridization and extension are followed by PCR

amplification and the amplicon is then finally quantified by microfluidic qPCR using Fluidigm BioMark HD system (Fluidigm Corporation, South San Francisco, CA). The Organ Damage panel (<https://www.olink.com/products/organ-damage-panel/>) was used in this study. It consists of 92 unique markers of toxicity and cellular damage. In the data post processing, we only included experiments with >65% of the samples above the limit of detection. The limit of detection is set at 3 standard deviation above negative control values.

Scanning Electron Microscopy

Freshly fabricated PDMS MPS were sputtered with gold/palladium (AuPd) for 60 s at 10 mA to get a 10 nm



conductive layer at the surface (Cressington sputter coater 108 auto, Watford, England, United Kingdom). The sample was then imaged in a scanning electron microscope (Quantum 3D FEG, Orion Nanofab, ZEISS, Oberkochen, Germany) with the following settings: 30 μm aperture, 20 kV, 120 pA, $\times 40^\circ$ tilt, $\times 1974$ magnification, 30 μs scan rate.

Statistics

All statistics were calculated using GraphPad Prism (San Diego, CA). All electrophysiology graphs statistics were analyzed with one-way ANOVA with Dunnett's post-hoc analysis and multiple comparison to dose 0 for HCQ and AZM. Multiple comparison to no drug and HCQ only was run for the AZM + HCQ combination acute drug study. One way ANOVA, multiple comparison to dose 0 and to one another with Dunnett's post-hoc analysis was also run on the Olink proteomics data. Non-parametric Chi-squared approximation was run for qualitative arrhythmic events assessment in a pairwise manner. Significance was determined with p -value < 0.05 . * $p < 0.05$; ** $p < 0.01$; *** $p < 0.001$, **** $p < 0.0001$.

RESULTS

Multiplexing of Cardiac Microphysiological System and Fluid Dynamic Modeling

We optimized our previously published cardiac MPS (Mathur et al., 2015) in a number of ways, including chamber design, cell composition, multiplexing and pressure driven fluidic pump. Cardiomyocyte function was optically recorded prior and during experiments with both voltage (BERST-1 voltage sensitive dye) and calcium transient (GCAMP encoded calcium sensor) reporters (Figure 1A). We added five

mechanosensing pillars of 20 μm diameter (Figure 1B, right) at the top and the bottom of the cell chamber to act as a resistance against which the tissue will exercise for enhanced tissue development and contraction force. The cell chamber dimensions were 1300 $\mu\text{m} \times 130 \mu\text{m}$ (Figure 1C). Absorption studies showed no significant drug binding to the microfluidic system for HCQ or AZM at any dose (Supplementary Figures 2A,B). These findings confirmed that the MPS were indeed exposed to intended concentrations. The free fraction of drug in our culture media was almost 90% for HCQ and 75% for AZM (Supplementary Figure 2C). Fluid mechanical characterization of the cardiac MPS was done *via* solving the Navier-Stokes equation using the finite element solver, COMSOL Multiphysics® (Burlington, MA, United States) to obtain the velocity (Figure 1D) as well as the wall shear stress (Figure 1E) profiles within the device. Our analyses show that the maximum values of velocity and wall shear stress within the MPS are 16 mm/s and 1.6 Pa ([6 dyn/cm², within the range of blood vessel wall shear stress (Koutsiaris et al., 2007)], respectively. Furthermore, the simulations confirmed that the cardiac tissue is protected from the media shear stress by the endothelial-like fenestration barrier (Mathur et al., 2015). The protective barrier also allows for rapid delivery of small molecules to the tissue, supplying a sufficient amount of nutrients throughout the study, as previously described (Mathur et al., 2015).

Acute Exposure to Hydroxychloroquine Triggers QT Prolongation and Rhythm Instability, Leading to Arrhythmic Events and Stop of Spontaneous Beating Activity

We performed a dose-escalation study for HCQ using the cardiac MPS. It is known that HCQ inhibits I_{Kr} potassium channels (also

named *hERG* channels) (Jankelson et al., 2020), triggering an increase in QT interval of cardiomyocytes. QT interval above 500 ms is typically correlated with arrhythmias that are responsible for sudden death (Jankelson et al., 2020). We observed an increase of APD₈₀ at the clinical C_{max} of 1 μM as well as an increase in the AP triangulation after 10 μM (Figures 2A,C). The beat frequency did not change with increasing HCQ dose (Figure 2B). The voltage upstroke velocity decreased at 10 μM, although not significantly (Figure 2D), while the calcium upstroke velocity showed a dramatic decrease with HCQ increasing dose, especially at 10 and 100 μM (Figure 2E). Rhythm instabilities were also observed in Poincaré plots for 67% of the tissues at 10 μM (Figure 2F). Interestingly, APD and triangulation increases were correlated with EADs (calcium traces) (Figure 3A). We observed arrhythmic events in 72% of the tissues at 100 μM and 22% at 10 μM, and 78% of tissues showed weak or no beating signal at 1000 μM (Figure 3D).

Acute Exposure to Azithromycin Triggers Rhythm Instability, Correlated to Arrhythmic Events and Stop of Spontaneous Beating Activity

We performed a dose-escalation study for AZM using the cardiac MPS. AZM is also associated with an increased risk of cardiac arrhythmia (Ray et al., 2012), although not necessarily related to QT increase (Yang et al., 2017; Roy and MainakMukhopadhyay, 2020). The APD₈₀ did not show any change up to 6.7 μM (10 × C_{max}) and decreased at 67 μM (Figure 4A). However, at 67 μM, only 12% of AZM-treated tissues were beating spontaneously (Figure 3E), and therefore, the decrease in APD₈₀ was most likely due to toxicity. We observed an increase in AP triangulation at 6.7 μM (Figure 4C). No significant change was seen in beating frequency (Figure 4B) or AP upstroke velocity (Figure 4D). Calcium transient upstroke velocity, however, showed a significant decrease starting at 6.7 μM (Figure 4E). We observed an increased rhythm instability starting at 0.67 μM (C_{max}) to 6.7 μM, where 60% of the tissues were unstable (Figure 4F). A typical arrhythmic observation in AZM arrhythmic MPS were delayed after depolarization (DAD, Figure 3B). Figure 3E shows that arrhythmic events occur in 75% of the tissues at 6.7 μM and by 67 μM 12% of tissues showed arrhythmias, while the remaining tissues had weak or no beating signal.

Acute Exposure of Hydroxychloroquine and Azithromycin Polytherapy Triggers Triangulation and Rhythm Instability, Which Correlated With Arrhythmic Events

As observed in HCQ alone data (Figure 2A), the addition of HCQ at C_{max} (1 μM) increased the APD₈₀ significantly (Figure 5A). Increasing concentrations of AZM were applied in combination with 1 μM HCQ and further increased the APD₈₀ up to the AZM C_{max} (0.67 μM). At HCQ +6.7 μM AZM the APD₈₀ reverted to the baseline value (Figure 5A), probably due to toxicity, as voltage signals became weak with arrhythmic events

(Figure 3F). No change was observed in beat frequency (Figure 5B). The AP triangulation did not show a significant increase with 1 μM HCQ alone; however, the addition of AZM increased it continuously until a significant change was observed at the highest dose (Figure 5C). The combination of both drugs decreased the upstroke velocity for both AP (Figure 5D) and calcium (Figure 5E). Poincaré plots showed first occurrences of instabilities with the addition of C_{max} HCQ (16% of MPS). The incidence of instabilities increased further with AZM concentrations until 70% of MPS showed instabilities at 0.67 μM AZM. (Figure 5F). APD lengthening accompanied with triangulation increase, also increased rhythm instabilities and triggered arrhythmic events. Interestingly, most arrhythmic outcomes were TdP-like events (Figure 3C), where traces changed shape and amplitude (not shown since the traces' amplitudes were normalized here), the plateau phase was absent and the signal became weak when compared to control traces. TdP are typically observed on ECG when traces continuously change configuration and amplitude (Asensio et al., 2020). We observed the appearance of arrhythmic events in 16% of the tissues starting with HCQ only and increasing to 33% with the addition of 0.67 μM AZM and 50% with 2 and 6.7 μM AZM. At the highest concentration, 30% of tissues showed weak or no beating signals (Figure 3F).

Proteomics Analysis of Microphysiological System Effluent Reveals Cardiotoxicity Biomarkers to be Potentially Monitored in Patients Treated With Hydroxychloroquine and/or Azithromycin

We analyzed the effluent from the cardiac MPS microfluidic channels for 92 biomarkers and report only biomarkers related to cardiotoxicity that changed significantly upon acute exposure to either HCQ or AZM alone and their combination. We observed a significant increase of VASH1 and GALNT10 (Figure 6A) at 100 μM HCQ when compared to 0 μM. Cardiac troponin I, TNNI3, a well-known biomarker of cardiac injury, showed a significant increase at 100 μM when compared to both 0 and 1 μM HCQ (Figure 6A). Acute AZM exposure showed a significant decrease in EPO (Erythropoietine) (Figure 6B) at 67 μM when compared to 0 μM. No biomarkers changed significantly in the highest dose of polytherapy (1 × C_{max} HCQ +10 × C_{max} AZM) compared to no drug or 1 × C_{max} HCQ alone. No change in TNNI3 was observed for both AZM and polytherapy (Figures 6B,C), suggesting that high HCQ doses are more cardiotoxic than high doses of AZM alone or in combination with HCQ at C_{max}.

DISCUSSION

Maximal AP upstroke velocity is a common measure of *I_{Na}* (Casini et al., 2009), and is an important metric to assess safety features of drugs; its dysfunction may cause life-threatening cardiac arrhythmias by reducing cardiac excitability (Tan et al., 2001; Chatre et al., 2018). Neither HCQ (Figure 2D) or AZM (Figure 4D) monotherapies

showed a significant change in cardiac I_{Na} . However, the polytherapy showed a synergistic decrease in the AP upstroke velocity when compared to monotherapies (**Figure 5D**). Interestingly, HCQ is a known I_{Na} blocker (Chatre et al., 2018) whereas AZM has been reported to potentiate cardiac I_{Na} (Yang et al., 2017), suggesting that HCQ-dependent block of I_{Na} dominates the effect of AZM on I_{Na} .

Maximal calcium upstroke velocity is directly correlated to the speed of sarcoplasmic reticulum Ca^{2+} release, executed by ryanodine receptors opening (RyR) (Jaimes et al., 2016). HCQ has been shown to facilitate the oxidation and dysfunction of RyR (Zhang et al., 2020), which negatively impacts calcium upstroke velocity. HCQ is also an I_{CaL} blocker (Capel et al., 2015), which will decrease both calcium transient upstroke velocity and amplitude (Grantham and Cannell, 1996). We identified a decrease in calcium upstroke velocity with HCQ acute exposure (**Figure 2E**). AZM-dependent I_{Na} potentiation can also promote intracellular sodium loading, and subsequently dysregulates intracellular calcium concentration, that will lead to DAD (Antzelevitch and Burashnikov, 2011) (**Figure 3B**), and a decrease in calcium transient upstroke velocity (**Figure 4E**). The polytherapy synergistically decreased the calcium transient upstroke velocity (**Figure 5E**), suggesting that an AZM-dependent I_{Na} potentiation is required in addition to 1 μ M HCQ to significantly decrease calcium upstroke velocity.

Increases in APD and triangulation, accompanied by instabilities (i.e., Poincaré plots), typically leads to arrhythmias (Hondeghem et al., 2001). HCQ has a known I_{Kr} block effect associated with QT prolongation and arrhythmic events (Sharma et al., 2016; Blinova et al., 2017; Jankelson et al., 2020). Our experimental action potential data are consistent with the clinical literature (Asensio et al., 2020; Bessière et al., 2020) and indicate that the cardiac MPS is a good predictor of the clinical cardiotoxicity of HCQ. Interestingly AZM has been associated with an increase in cardiovascular death, mostly through QT prolongation and arrhythmia (Ray et al., 2012; Vouri et al., 2021). However, it has also been shown that AZM lacks strong pharmacodynamic evidence of I_{Kr} inhibition, and that it can cause ventricular tachycardia in the absence of QT prolongation, indicating a novel proarrhythmic syndrome (Yang et al., 2017). This novel syndrome was successfully observed in our cardiac MPS: unchanged APD₈₀ up to 6.7 μ M AZM, with increased instabilities and arrhythmic events. The AZM data clearly show that the cardiac MPS can predict arrhythmias through beat shape changes (triangulation increase) and instabilities, even in the absence of APD₈₀ prolongation. The latter is important for critical arrhythmia prediction and has been a focus of revised International Conference on Harmonization (ICH) E14 recommendations by both the CiPA initiative (Dutta et al., 2017a; Dutta et al., 2017b) and the pharmaceutical industry. The E14 guidance is intended to encourage the assessment of drug effects on the QT/QTc interval as a standard part of drug safety evaluation (Food and Drug Administration, 2005).

The polytherapy study showed a significant increase of APD₈₀, triangulation and instability as AZM dose was escalated in presence of a constant HCQ concentration, supporting literature that observed a worsening of QT interval increase

with combination therapy (Chorin et al., 2020a; Chorin et al., 2020b; Bessière et al., 2020; Mercurio et al., 2020). In polytherapy we observed arrhythmia in 30–50% of the tissues at C_{max} HCQ + C_{max} AZM, corresponding to clinical data where 75% of patients who were given a combination of HCQ and AZM had ventricular arrhythmias (Gérard et al., 2020). Despite the presence of arrhythmic behavior, we did not see a significant change in arrhythmia instances when comparing C_{max} HCQ to C_{max} HCQ + AZM in polytherapy recordings. The latter suggests no worsening of arrhythmic behavior when AZM was added to C_{max} HCQ. This is in concordance with clinical data, concluding that there were no significant differences in the relative likelihood of abnormal ECG findings for polytherapy compared to monotherapy (Rosenberg et al., 2020).

The biomarker study showed an increase in numerous cardiotoxicity-related proteins when tissues were exposed to HCQ (**Figure 6A**). The marker VASH1 is associated with stiffer cardiac tissues and slower relaxation of failing human cardiomyocytes (Chen et al., 2020). GALNT10 has a critical role in protein folding, secretion and stability. Its upregulation has been shown to be a reparative response in mice 5 days post myocardial infarction (Hunt et al., 2012). Finally, a significant increase in cardiac troponin I (TNNI3), a well-known biomarker of cardiac injury (Sandoval et al., 2020; Lindner et al., 2020), correlates well with our observations of cardiotoxic effects of HCQ as well as clinically reported HCQ-related troponin I increase (Joyce et al., 2013). AZM exposure significantly decreased EPO (**Figure 6B**), which is indicative of cardiotoxicity (Santhanam et al., 2010). In cardiomyocytes, GALNT10 is typically an intracellular protein, suggesting cellular damage of the tissues at high doses of HCQ. No biomarkers changed significantly in the highest dose of polytherapy (C_{max} HCQ + 10 \times C_{max} AZM) compared to no drug or C_{max} HCQ alone (**Figure 6C**). This matches with results of single drug experiments, where significant changes were only observed for very high doses (100 \times C_{max}) of the respective drug. Additional analysis will be needed to identify more subtle biomarker changes at lower drug concentrations.

In the 12 months following the official declaration of global pandemic in March 2020, emergency use authorization of drugs like HCQ and AZM have been granted and revoked, due to inconclusive efficacy of the drugs to reduce viral load. In 250 clinical trials that were started, with significant costs and resources of the healthcare system, many studies had inconclusive efficacy outcomes or were terminated due to cardiac liability issues. If used prospectively, our MPS would have successfully predicted the clinical cardiology response (Chorin et al., 2020a; Asensio et al., 2020; Chorin et al., 2020b; Bessière et al., 2020; Mercurio et al., 2020), in that the combination of both drugs would synergistically increase QT interval when compared to single drug exposure, while not impacting the overall frequency of arrhythmic events. Furthermore, by combining the cardiac MPS with *in silico* methods we can address mechanism of action, at an ion channel level, of potential drug side effects and better predict drug effectiveness (Tveito et al., 2018; Jæger et al., 2020b; Jæger et al., 2021). Thus,

employing cardiac MPS prior to clinical trials would enable rapid evaluation of the cardiac safety of promising drug candidates and drug combinations.

CONCLUSION

Our cardiac MPS, containing a 3D human heart muscle, can predict arrhythmic risk based on the observation of triangulation changes and instabilities, even if such arrhythmias occur in the absence of action potential duration prolongation. The methodology of this study can be extended to novel more promising therapeutics to treat COVID-19, and to MPS representing a disease state of the cardiac muscle. The high content, controlled and inexpensive MPS should help to rapidly evaluate safety properties of potential therapeutics in crisis times, and accelerate clinical decision making.

DATA AVAILABILITY STATEMENT

The raw data supporting the conclusion of this article will be made available by the authors, without undue reservation.

ETHICS STATEMENT

The studies involving human iPSCs were reviewed and approved by the UC Berkeley Stem Cell Oversight Committee.

AUTHOR CONTRIBUTIONS

All authors participated in the study design, analysis of the data, interpretation of the results and review of the manuscript; BC and VC conducted the main experiments, device fabrication and qualitative EAD characterization; BS performed the cell culture

REFERENCES

- Andrea Natale, M. (2020). Prophylactic Benefit of Hydroxychloroquine in COVID-19 Cases with Mild to Moderate Symptoms and in Healthcare Workers with High Exposure Risk: *clinicaltrials.gov*. [Available at: <https://www.clinicaltrials.gov/ct2/show/study/NCT04371926?term=hydroxychloroquine&recrs=i&cond=Covid19&draw=2&rank=7>].
- Antzelevitch, C., and Burashnikov, A. (2011). Overview of Basic Mechanisms of Cardiac Arrhythmia. *Card. Electrophysiol. Clin.* 3 (1), 23–45. doi:10.1016/j.jcep.2010.10.012
- Asensio, E., Acunzo, R., Uribe, W., Saad, E. B., and Sáenz, L. C. (2020). Recommendations for the Measurement of the QT Interval during the Use of Drugs for COVID-19 Infection Treatment. Updatable in Accordance with the Availability of New Evidence. *J. Interv. Card. Electrophysiol.* 59 (2), 315–320. doi:10.1007/s10840-020-00765-3
- Assarsson, E., Lundberg, M., Holmquist, G., Björkstén, J., Thorsen, S. B., Ekman, D., et al. (2014). Homogenous 96-plex PEA Immunoassay Exhibiting High Sensitivity, Specificity, and Excellent Scalability. *PLoS One* 9 (4), e95192. doi:10.1371/journal.pone.0095192
- Bessière, F., Rocchia, H., Delinière, A., Charrière, R., Chevalier, P., Argaud, L., et al. (2020). Assessment of QT Intervals in a Case Series of Patients with Coronavirus

and helped with MPS preparation and maintenance; AE helped with interpretation of electrophysiological recordings; IG performed computational characterization of fluid flow within the MPS; HF developed and provided the Python script for data analysis and helped with trace evaluation; IR, CS, and Y-SL analyzed drug absorption and free drug concentrations; EWM provided BeRST-1 dye; BC, VC, AE, and KH wrote the manuscript; BC prepared the figures and caption; KH funded the work.

FUNDING

This work was funded in part by the California Institute for Regenerative Medicine DISC2-10090 and DISC2P-11946 (KEH), NIH-NHLBI HL130417 (KEH), NIH-NIGMS R35GM119855 (EWM), and the Peder Sather Center for Advanced Study (UC Berkeley).

ACKNOWLEDGMENTS

We thank Bruce Conklin (Gladstone Institutes, San Francisco, United States) for technical advice on the WTC iPSC line and Samuel Wall (Simula Research Laboratory, Oslo, Norway) for providing the scripts to analyze action potential waveforms and Poincaré plots. We thank the Marvel Nanofabrication laboratory (UC Berkeley) and their staff for assistance and technical advice for microfabrication procedures.

SUPPLEMENTARY MATERIAL

The Supplementary Material for this article can be found online at: <https://www.frontiersin.org/articles/10.3389/fphar.2021.684252/full#supplementary-material>

- Disease 2019 (COVID-19) Infection Treated with Hydroxychloroquine Alone or in Combination with Azithromycin in an Intensive Care Unit. *JAMA Cardiol.* 5 (9), 1067–1069. doi:10.1001/jamacardio.2020.1787
- Blinova, K., Stohlman, J., Vicente, J., Chan, D., Johannesen, L., Hortigon-Vinagre, M. P., et al. (2017). Comprehensive Translational Assessment of Human-Induced Pluripotent Stem Cell Derived Cardiomyocytes for Evaluating Drug-Induced Arrhythmias. *Toxicol. Sci.* 155 (1), 234–247. doi:10.1093/toxsci/kfw200
- Burgos, R. M., Badowski, M. E., Drwiega, E., Ghassemi, S., Griffith, N., Herald, F., et al. (2021). The Race to a COVID-19 Vaccine: Opportunities and Challenges in Development and Distribution. *Drugs Context* 10, 10. doi:10.7573/dic.2020-12-2
- Capel, R. A., Herring, N., Kalla, M., Yavari, A., Mirams, G. R., Douglas, G., et al. (2015). Hydroxychloroquine Reduces Heart Rate by Modulating the Hyperpolarization-Activated Current if: Novel Electrophysiological Insights and Therapeutic Potential. *Heart Rhythm* 12 (10), 2186–2194. doi:10.1016/j.hrthm.2015.05.027
- Casini, S., Verkerk, A. O., Van Borren, M. M. G. J., Van Ginneken, A. C. G., Veldkamp, M. W., De Bakker, J. M. T., et al. (2009). Intracellular Calcium Modulation of Voltage-Gated Sodium Channels in Ventricular Myocytes. *Cardiovasc. Res.* 81 (1), 72–81. doi:10.1093/cvr/cvn274
- Charrez, B., Charwat, V., Siemons, B., Finsberg, H., Miller, E. W., Edwards, A. G., et al. (2021). *In Vitro* safety "clinical Trial" of the Cardiac Liability of Drug Polytherapy. *Clin. Transl. Sci.* 14 (3), 1155–1165. doi:10.1111/cts.13038

- Chatre, C., Roubille, F., Vernhet, H., Jorgensen, C., and Pers, Y.-M. (2018). Cardiac Complications Attributed to Chloroquine and Hydroxychloroquine: A Systematic Review of the Literature. *Drug Saf.* 41 (10), 919–931. doi:10.1007/s40264-018-0689-4
- Chen, C. Y., Salomon, A. K., Caporizzo, M. A., Curry, S., Kelly, N. A., Bedi, K., et al. (2020). Depletion of Vasohibin 1 Speeds Contraction and Relaxation in Failing Human Cardiomyocytes. *Circ. Res.* 127 (2), e14–e27. doi:10.1161/circresaha.119.315947
- Chorin, E., Dai, M., Shulman, E., Wadhvani, L., Bar-Cohen, R., Barbhayai, C., et al. (2020). The QT Interval in Patients with COVID-19 Treated with Hydroxychloroquine and Azithromycin. *Nat. Med.* 26 (6), 808–809. doi:10.1038/s41591-020-0888-2
- Chorin, E., Wadhvani, L., Magnani, S., Dai, M., Shulman, E., Nadeau-Routhier, C., et al. (2020). QT interval prolongation and torsades de pointes in patients with COVID-19 treated with hydroxychloroquine/azithromycin. *Heart Rhythm* 17 (9), 1425–1433. doi:10.1016/j.hrthm.2020.05.014
- Dunn, K. K., and Palecek, S. P. (2018). Engineering Scalable Manufacturing of High-Quality Stem Cell-Derived Cardiomyocytes for Cardiac Tissue Repair. *Front. Med.* 5, 110. doi:10.3389/fmed.2018.00110
- Dutta, S., Chang, K. C., Beattie, K. A., Sheng, J., Tran, P. N., Wu, W. W., et al. (2017). Corrigendum: Optimization of an In Silico Cardiac Cell Model for Proarrhythmia Risk Assessment. *Front. Physiol.* 8, 1025. doi:10.3389/fphys.2017.01025
- Dutta, S., Chang, K. C., Beattie, K. A., Sheng, J., Tran, P. N., Wu, W. W., et al. (2017). Optimization of an In Silico Cardiac Cell Model for Proarrhythmia Risk Assessment. *Front. Physiol.* 8, 616. doi:10.3389/fphys.2017.00616
- FDA (2020a). FDA Approves First Treatment for COVID-19. [Available at: <https://www.fda.gov/news-events/press-announcements/fda-approves-first-treatment-covid-19>].
- FDA (2020b). FDA Cautions against Use of Hydroxychloroquine or Chloroquine for COVID-19 outside of the Hospital Setting or a Clinical Trial Due to Risk of Heart Rhythm Problems. [Available at: <https://www.fda.gov/drugs/drug-safety-and-availability/fda-cautions-against-use-hydroxychloroquine-or-chloroquine-covid-19-outside-hospital-setting-or>].
- FDA (2020c). Request for Emergency Use Authorization for Use of Chloroquine Phosphate or Hydroxychloroquine Sulfate Supplied from the Strategic National Stockpile for Treatment of 2019 Coronavirus Disease. [Available at: <https://www.fda.gov/media/136534/download>].
- Food and Drug Administration H (2005). International Conference on Harmonisation; Guidance on E14 Clinical Evaluation of QT/QTc Interval Prolongation and Proarrhythmic Potential for Non-antiarrhythmic Drugs; Availability. *Notice. Fed. Regist.* 70, 61134–61135.
- Furtado, R. H. M., Berwanger, O., Fonseca, H. A., Corrêa, T. D., Ferraz, L. R., Lapa, M. G., et al. (2020). Azithromycin in Addition to Standard of Care versus Standard of Care Alone in the Treatment of Patients Admitted to the Hospital with Severe COVID-19 in Brazil (COALITION II): a Randomised Clinical Trial. *The Lancet* 396 (10256), 959–967. doi:10.1016/s0140-6736(20)31862-6
- Gautret, P., Lagier, J.-C., Parola, P., Hoang, V. T., Meddeb, L., Mailhe, M., et al. (2020). Hydroxychloroquine and Azithromycin as a Treatment of COVID-19: Results of an Open-Label Non-randomized Clinical Trial. *Int. J. Antimicrob. Agents* 56 (1), 105949. doi:10.1016/j.ijantimicag.2020.105949
- Gérard, A., Romani, S., Fresse, A., Viard, D., Parassol, N., Granvullemin, A., et al. (2020). "Off-label" Use of Hydroxychloroquine, Azithromycin, Lopinavir-Ritonavir and Chloroquine in COVID-19: A Survey of Cardiac Adverse Drug Reactions by the French Network of Pharmacovigilance Centers. *Therapies* 75 (4), 371–379. doi:10.1016/j.therap.2020.05.002
- Grantham, C. J., and Cannell, M. B. (1996). Ca²⁺ Influx during the Cardiac Action Potential in Guinea Pig Ventricular Myocytes. *Circ. Res.* 79 (2), 194–200. doi:10.1161/01.res.79.2.194
- Hondeghem, L. M., Carlsson, L., and Duker, G. (2001). Instability and Triangulation of the Action Potential Predict Serious Proarrhythmia, but Action Potential Duration Prolongation Is Antiarrhythmic. *Circulation* 103 (15), 2004–2013. doi:10.1161/01.cir.103.15.2004
- Huang, M., Tang, T., Pang, P., Li, M., Ma, R., Lu, J., et al. (2020). Treating COVID-19 with Chloroquine. *J. Mol. Cell Biol* 12 (4), 322–325. doi:10.1093/jmcb/mjaa014
- Huang, Y.-L., Walker, A. S., and Miller, E. W. (2015). A Photostable Silicon Rhodamine Platform for Optical Voltage Sensing. *J. Am. Chem. Soc.* 137 (33), 10767–10776. doi:10.1021/jacs.5b06664
- Huebsch, N., Charrez, B., Siemons, B., Boggess, S. C., Wall, S., Neiman, G., et al. (2020). Metabolically-Driven Maturation of hiPSC-Cell Derived Cardiac Chip. *bioRxiv*, 485169. doi:10.1101/485169
- Huebsch, N., Loskill, P., Mandegar, M. A., Marks, N. C., Sheehan, A. S., Ma, Z., et al. (2015). Automated Video-Based Analysis of Contractility and Calcium Flux in Human-Induced Pluripotent Stem Cell-Derived Cardiomyocytes Cultured over Different Spatial Scales. *Tissue Eng. C: Methods* 21 (5), 467–479. doi:10.1089/ten.tec.2014.0283
- Hunt, D. L., Campbell, P. H., Zambon, A. C., Vranizan, K., Evans, S. M., Kuo, H.-C., et al. (2012). Early Postmyocardial Infarction Survival in Murphy Roths Large Mice Is Mediated by Attenuated Apoptosis and Inflammation but Depends on Genetic Background. *Exp. Physiol.* 97 (1), 102–114. doi:10.1113/expphysiol.2011.060269
- Jäger, K. H., Charwat, V., Charrez, B., Finsberg, H., Maleckar, M. M., Wall, S., et al. (2020). Improved Computational Identification of Drug Response Using Optical Measurements of Human Stem Cell Derived Cardiomyocytes in Microphysiological Systems. *Front. Pharmacol.* 10, 1648. doi:10.3389/fphar.2019.01648
- Jäger, K. H., Charwat, V., Wall, S., Healy, K. E., and Tveito, A. (2020). Identifying Drug Response by Combining Measurements of the Membrane Potential, the Cytosolic Calcium Concentration, and the Extracellular Potential in Microphysiological Systems. *Front. Pharmacol.* 11 (2085), 569489. doi:10.3389/fphar.2020.569489
- Jäger, K. H., Charwat, V., Wall, S., Healy, K. E., and Tveito, A. (2021). Identifying Drug Response by Combining Measurements of the Membrane Potential, the Cytosolic Calcium Concentration, and the Extracellular Potential in Microphysiological Systems. *Front. Pharmacol.* 11 (2085), 569489. doi:10.3389/fphar.2020.569489
- Jaimes, R., Walton, R. D., Pasdois, P., Bernus, O., Efimov, I. R., and Kay, M. W. (2016). A Technical Review of Optical Mapping of Intracellular Calcium within Myocardial Tissue. *Am. J. Physiology-Heart Circulatory Physiol.* 310 (11), H1388–H1401. doi:10.1152/ajpheart.00665.2015
- Jankelson, L., Karam, G., Becker, M. L., Chinitz, L. A., and Tsai, M.-C. (2020). QT prolongation, torsades de pointes, and sudden death with short courses of chloroquine or hydroxychloroquine as used in COVID-19: A systematic review. *Heart Rhythm* 17 (9), 1472–1479. doi:10.1016/j.hrthm.2020.05.008
- JHU (2020). COVID-19 Dashboard by the Center for Systems Science and Engineering (CSSE). Available at: <https://coronavirus.jhu.edu/map.html> Johns Hopkins University.
- Joyce, E., Fabre, A., and Mahon, N. (2013). Hydroxychloroquine Cardiotoxicity Presenting as a Rapidly Evolving Biventricular Cardiomyopathy: Key Diagnostic Features and Literature Review. *Eur. Heart J. Acute Cardiovasc. Care* 2 (1), 77–83. doi:10.1177/2048872612471215
- Koutsisaris, A. G., Tachmitzi, S. V., Batis, N., Kotoula, M. G., Karabatsas, C. H., Tsironi, E., et al. (2007). Volume Flow and wall Shear Stress Quantification in the Human Conjunctival Capillaries and post-capillary Venules *In Vivo*. *Biorheology* 44 (5-6), 375–386.
- Lian, X., Bao, X., Al-Ahmad, A., Liu, J., Wu, Y., Dong, W., et al. (2014). Efficient Differentiation of Human Pluripotent Stem Cells to Endothelial Progenitors via Small-Molecule Activation of WNT Signaling. *Stem Cell Rep.* 3 (5), 804–816. doi:10.1016/j.stemcr.2014.09.005
- Lian, X., Zhang, J., Azarin, S. M., Zhu, K., Hazeltine, L. B., Bao, X., et al. (2013). Directed Cardiomyocyte Differentiation from Human Pluripotent Stem Cells by Modulating Wnt/ β -Catenin Signaling under Fully Defined Conditions. *Nat. Protoc.* 8 (1), 162–175. doi:10.1038/nprot.2012.150
- Lindner, D., Fitzek, A., Bräuninger, H., Aleshcheva, G., Edler, C., Meissner, K., et al. (2020). Association of Cardiac Infection with SARS-CoV-2 in Confirmed COVID-19 Autopsy Cases. *JAMA Cardiol.* 5 (11), 1281–1285. doi:10.1001/jamacardio.2020.3551
- Mathur, A., Loskill, P., Shao, K., Huebsch, N., Hong, S., Marcus, S. G., et al. (2015). Human iPSC-Based Cardiac Microphysiological System for Drug Screening Applications. *Sci. Rep.* 5, 8883. doi:10.1038/srep08883
- Mercuro, N. J., Yen, C. F., Shim, D. J., Maher, T. R., McCoy, C. M., Zimetbaum, P. J., et al. (2020). Risk of QT Interval Prolongation Associated with Use of Hydroxychloroquine with or without Concomitant Azithromycin Among Hospitalized Patients Testing Positive for Coronavirus Disease 2019 (COVID-19). *JAMA Cardiol.* 5 (9), 1036–1041. doi:10.1001/jamacardio.2020.1834

- Molina, J. M., Delaugerre, C., Le Goff, J., Mela-Lima, B., Ponscarne, D., Goldwirt, L., et al. (2020). No Evidence of Rapid Antiviral Clearance or Clinical Benefit with the Combination of Hydroxychloroquine and Azithromycin in Patients with Severe COVID-19 Infection. *Médecine et Maladies Infectieuses* 50 (4), 384. doi:10.1016/j.medmal.2020.03.006
- Nishiga, M., Wang, D. W., Han, Y., Lewis, D. B., and Wu, J. C. (2020). COVID-19 and Cardiovascular Disease: from Basic Mechanisms to Clinical Perspectives. *Nat. Rev. Cardiol.* 17, 543–558. doi:10.1038/s41569-020-0413-9
- Perez-Bermejo, J. A., Kang, S., Rockwood, S. J., Simoneau, C. R., Joy, D. A., Ramadoss, G. N., et al. (2020). SARS-CoV-2 Infection of Human iPSC-Derived Cardiac Cells Predicts Novel Cytopathic Features in Hearts of COVID-19 Patients. *bioRxiv*. 25.265561. doi:10.1101/2020.08.25.265561
- Qu, Z., Xie, L.-H., Olcese, R., Karagueuzian, H. S., Chen, P.-S., Garfinkel, A., et al. (2013). Early Afterdepolarizations in Cardiac Myocytes: beyond Reduced Repolarization reserve. *Cardiovasc. Res.* 99 (1), 6–15. doi:10.1093/cvr/cvt104
- Randall, T. (2021). When Will Life Return to Normal? 7 Years at Today's Vaccine Rates: *Bloomberg.Com*. [Available from: <https://www.bloomberg.com/news/articles/2021-02-04/when-will-covid-pandemic-end-near-me-vaccine-coverage-calculator>].
- Ray, W. A., Murray, K. T., Hall, K., Arbogast, P. G., and Stein, C. M. (2012). Azithromycin and the Risk of Cardiovascular Death. *N. Engl. J. Med.* 366 (20), 1881–1890. doi:10.1056/nejmoa1003833
- Rosenberg, E. S., Dufort, E. M., Udo, T., Wilberschied, L. A., Kumar, J., Tesoriero, J., et al. (2020). Association of Treatment with Hydroxychloroquine or Azithromycin with In-Hospital Mortality in Patients with COVID-19 in New York State. *JAMA* 323 (24), 2493–2502. doi:10.1001/jama.2020.8630
- Roy, S., and Mukhopadhyay, M. (2020). Ventricular Arrhythmia Risk Based on Ethnicity in COVID-19 Patients on Hydroxychloroquine and Azithromycin Combination: Viewpoint. *SN Compr. Clin. Med.*, 1–6. doi:10.1007/s42399-020-00370-5
- Rupesh Agrawal, M. (2020). Safety and Efficacy of Hydroxychloroquine for at Risk Population (SHARP) against COVID-19. [Available at: <https://www.clinicaltrials.gov/ct2/show/study/NCT04342156?term=hydroxychloroquine&recrs=i&cond=Covid19&draw=2&rank=18>].
- Sandoval, Y., Januzzi, J. L., and Jaffe, A. S. (2020). Cardiac Troponin for Assessment of Myocardial Injury in COVID-19. *J. Am. Coll. Cardiol.* 76 (10), 1244–1258. doi:10.1016/j.jacc.2020.06.068
- Santhanam, A. V. R., D'Uscio, L. V., and Katusic, Z. S. (2010). Cardiovascular Effects of Erythropoietin. *Cardiovascular Pharmacology - Endothelial Control*. Elsevier, 257–285. doi:10.1016/b978-0-12-385061-4.00009-x
- Sanyaolu, A., Okorie, C., Marinkovic, A., Patidar, R., Younis, K., Desai, P., et al. (2020). Comorbidity and its Impact on Patients with COVID-19. *SN Compr. Clin. Med.* 2, 1–8. doi:10.1007/s42399-020-00363-4
- Sato, D., Xie, L.-H., Sovari, A. A., Tran, D. X., Morita, N., Xie, F., et al. (2009). Synchronization of Chaotic Early Afterdepolarizations in the Genesis of Cardiac Arrhythmias. *Proc. Natl. Acad. Sci.* 106 (9), 2983–2988. doi:10.1073/pnas.0809148106
- Self, W. H., Semler, M. W., Leather, L. M., Casey, J. D., Angus, D. C., Brower, R. G., et al. (2020). Effect of Hydroxychloroquine on Clinical Status at 14 Days in Hospitalized Patients with COVID-19: A Randomized Clinical Trial. *JAMA* 324, 2165–2176. doi:10.1001/jama.2020.22240
- Sharma, T. S., Wasko, M. C., Tang, X., Vedamurthy, D., Yan, X., Cote, J., et al. (2016). Hydroxychloroquine Use Is Associated with Decreased Incident Cardiovascular Events in Rheumatoid Arthritis Patients. *J. Am. Heart Assoc.* 5 (1), e002867. doi:10.1161/jaha.115.002867
- Ssentongo, P., Ssentongo, A. E., Heilbrunn, E. S., Ba, D. M., and Chinchilli, V. M. (2020). Association of Cardiovascular Disease and 10 Other Pre-existing Comorbidities with COVID-19 Mortality: A Systematic Review and Meta-Analysis. *PLoS One* 15 (8), e0238215. doi:10.1371/journal.pone.0238215
- Tan, H. L., Bink-Boelkens, M. T. E., Bezzina, C. R., Viswanathan, P. C., Beaufort-Krol, G. C. M., van Tintelen, P. J., et al. (2001). A Sodium-Channel Mutation Causes Isolated Cardiac Conduction Disease. *Nature* 409, 1043–1047. doi:10.1038/35059090
- Thomson, K., and Nachlis, H. (2020). Emergency Use Authorizations during the COVID-19 Pandemic. *Jama* 324, 1282–1283. doi:10.1001/jama.2020.16253
- Tohyama, S., Hattori, F., Sano, M., Hishiki, T., Nagahata, Y., Matsuura, T., et al. (2013). Distinct Metabolic Flow Enables Large-Scale Purification of Mouse and Human Pluripotent Stem Cell-Derived Cardiomyocytes. *Cell Stem Cell* 12 (1), 127–137. doi:10.1016/j.stem.2012.09.013
- Tveito, A., Jaeger, K. H., Huebsch, N., Charrez, B., Edwards, A. G., Wall, S., et al. (2018). Inversion and Computational Maturation of Drug Response Using Human Stem Cell Derived Cardiomyocytes in Microphysiological Systems. *Sci. Rep.* 8 (1), 17626. doi:10.1038/s41598-018-35858-7
- Vandenberk, B., Vandael, E., Robyns, T., Vandenberghe, J., Garweg, C., Foulon, V., et al. (2016). Which QT Correction Formulae to Use for QT Monitoring?. *J. Am. Heart Assoc.* 5 (6), e003264. doi:10.1161/jaha.116.003264
- Vouri, S. M., Thai, T. N., and Winterstein, A. G. (2021). An Evaluation of Co-use of Chloroquine or Hydroxychloroquine Plus Azithromycin on Cardiac Outcomes: A Pharmacoepidemiological Study to Inform Use during the COVID19 Pandemic. *Res. Soc. Administrative Pharm.* 17 (1), 2012–2017. doi:10.1016/j.sapharm.2020.04.031
- Wang, M., Cao, R., Zhang, L., Yang, X., Liu, J., Xu, M., et al. (2020). Remdesivir and Chloroquine Effectively Inhibit the Recently Emerged Novel Coronavirus (2019-nCoV) *In Vitro*. *Cell Res* 30 (3), 269–271. doi:10.1038/s41422-020-0282-0
- World Health Organization (2020). WHO Recommends against the Use of Remdesivir in COVID-19 Patients. [Available from: <https://www.who.int/news-room/feature-stories/detail/who-recommends-against-the-use-of-remdesivir-in-covid-19-patients>].
- Yang, Z., Prinsen, J. K., Bersell, K. R., Shen, W., Yermalitskaya, L., Sidorova, T., et al. (2017). Azithromycin Causes a Novel Proarrhythmic Syndrome. *Circ. Arrhythm Electrophysiol.* 10 (4), e003560. doi:10.1161/CIRCEP.115.003560
- Yao, X., Ye, F., Zhang, M., Cui, C., Huang, B., Niu, P., et al. (2020). *In Vitro* Antiviral Activity and Projection of Optimized Dosing Design of Hydroxychloroquine for the Treatment of Severe Acute Respiratory Syndrome Coronavirus 2 (SARS-CoV-2). *Clin. Infect. Dis.* 71 (15), 732–739. doi:10.1093/cid/ciaa237In
- Zhang, X.-L., Li, Z.-M., Ye, J.-T., Lu, J., Ye, L. L., Zhang, C.-X., et al. (2020). Pharmacological and Cardiovascular Perspectives on the Treatment of COVID-19 with Chloroquine Derivatives. *Acta Pharmacol. Sin* 41 (11), 1377–1386. doi:10.1038/s41401-020-00519-x

Conflict of Interest: KH and BS are part-time employed by the company Organos Inc. AE serves as an advisor to Organos Inc. with equity compensation. HF holds equity in Organos Inc.

The remaining authors declare that the research was conducted in the absence of any commercial or financial relationships that could be construed as a potential conflict of interest.

Publisher's Note: All claims expressed in this article are solely those of the authors and do not necessarily represent those of their affiliated organizations, or those of the publisher, the editors and the reviewers. Any product that may be evaluated in this article, or claim that may be made by its manufacturer, is not guaranteed or endorsed by the publisher.

Copyright © 2021 Charrez, Charwat, Siemons, Goswami, Sakolish, Luo, Finsberg, Edwards, Miller, Rusyn and Healy. This is an open-access article distributed under the terms of the Creative Commons Attribution License (CC BY). The use, distribution or reproduction in other forums is permitted, provided the original author(s) and the copyright owner(s) are credited and that the original publication in this journal is cited, in accordance with accepted academic practice. No use, distribution or reproduction is permitted which does not comply with these terms.